

# Lipid Compositions in Infant Formulas Affect the Solubilization of Antimalarial Drugs Artefenomel (OZ439) and Ferroquine during Digestion

Malinda Salim, Gisela Ramirez, Kang-Yu Peng, Andrew J. Clulow, Adrian Hawley, Hanu Ramachandrani, Stephane Beilles, and Ben J. Boyd\*



Cite This: *Mol. Pharmaceutics* 2020, 17, 2749–2759



Read Online

ACCESS |



Metrics & More



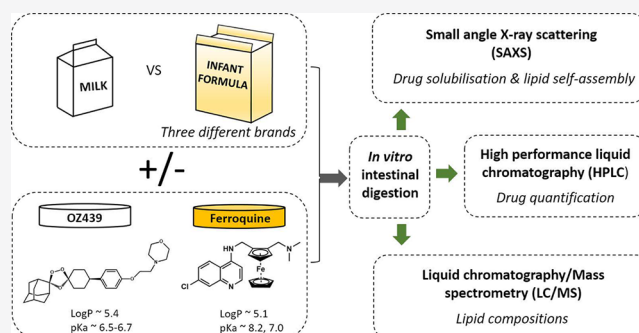
Article Recommendations



Supporting Information

**ABSTRACT:** Recent studies have shown that the solubilization of two antimalarial drug candidates, artefenomel (OZ439) and ferroquine (FQ), designed to provide a single-dose combination therapy for uncomplicated malaria can be enhanced using milk as a lipid-based formulation. However, milk as an excipient faces significant quality and regulatory hurdles. We therefore have investigated infant formula as a potential alternative formulation approach. The significance of the lipid species present in a formula with different lipid compositions upon the solubilization of OZ439 and FQ during digestion has been investigated. Synchrotron small-angle X-ray scattering was used to measure the diffraction from a dispersed drug during digestion and thereby determine the extent of drug solubilization. High-performance liquid chromatography was used to quantify the amount of drug partitioned into the digested lipid phases. Our results show that both the lipid species and the amount of lipids administered were key determinants for the solubilization of OZ439, while the solubilization of FQ was independent of the lipid composition. Infant formulas could therefore be designed and used as milk substitutes to tailor the desired level of drug solubilization while circumventing the variability of components in naturally derived milk. The enhanced solubilization of OZ439 was achieved during the digestion of medium-chain triacylglycerols (MCT), indicating the potential applicability of MCT-fortified infant formula powder as a lipid-based formulation for the oral delivery of OZ439 and FQ.

**KEYWORDS:** OZ439, ferroquine, milk, infant formula, lipid compositions, drug solubilization, *in vitro* digestion, X-ray scattering



## 1. INTRODUCTION

Lipid-based formulations (LBF) are one of the most widely used strategies to improve oral bioavailability of poorly water-soluble drugs by enhancing the dissolution of drugs in the gastrointestinal (GI) tract, prolonging the gastric retention time and potentially reducing the activity of efflux transporters on the intestinal wall.<sup>1</sup> Milk is a natural LBF where the lipids (~98% triacylglycerols, TAGs) are emulsified in an aqueous solution as milk fat globules that can be digested by the action of pancreatic lipase in the small intestine to form diacylglycerols (DAGs), monoacylglycerols (MAGs), and free fatty acids (FFAs).<sup>2,3</sup> These amphiphilic lipolytic products can self-assemble into liquid crystalline colloidal structures<sup>4,5</sup> and support the solubilization of poorly water-soluble drugs;<sup>6–9</sup> however, the types of the colloidal phases formed can also be influenced by the dosage and the physicochemical properties of the coadministered drugs.<sup>8,9</sup>

We have recently shown that the solubilization of the antimalarial drugs artefenomel (OZ439) and ferroquine (FQ) was enhanced during digestion in full-cream bovine milk,<sup>8,9</sup>

which was analogous to the results of bioavailability studies.<sup>10–12</sup> Although the positive effects of milk on the solubilization of OZ439 and FQ during intestinal lipolysis were clear, the use of milk and its practical application for oral coadministration with drugs in developing countries are limited by challenges. These include the need to refrigerate the milk prior to consumption and the presence of variations in the quality of milk, which will make its implementation as a Food and Drug Administration (FDA)-approved excipient for drug delivery difficult.<sup>13,14</sup> Therefore, powdered milk substitutes such as infant formulas may provide an alternative solution to the limited shelf life of fresh milk and offer a well-

Received: May 1, 2020  
Revised: June 1, 2020  
Accepted: June 2, 2020  
Published: June 23, 2020



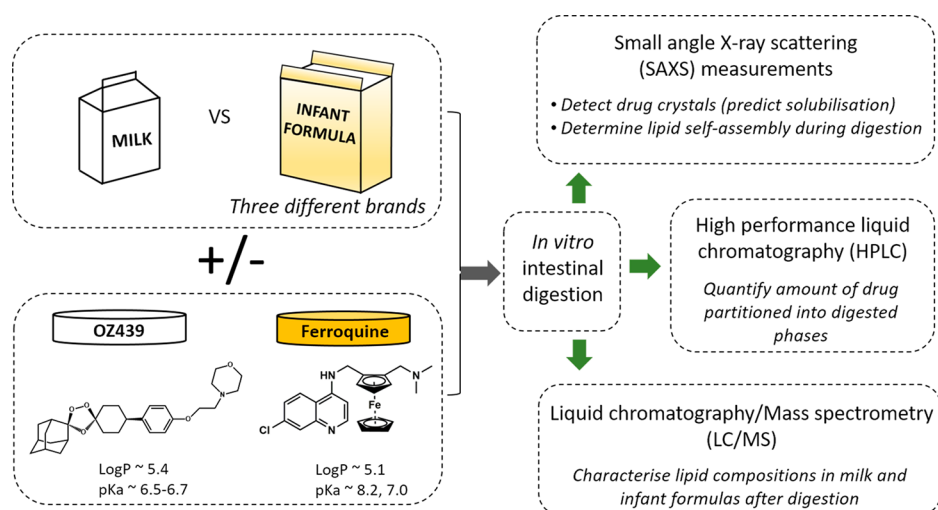


**Figure 1.** Schematic representation of the concept of this study.

controlled, consistent batch-to-batch quality of the lipid excipients.

Infant formulas are generally formulated using vegetable oil blends with or without bovine milk fat and are enriched with long-chain polyunsaturated fatty acids to improve the cognitive development of infants.<sup>15</sup> Although infant formulas are often designed based on the lipid compositions of human milk, a number of studies have shown that compositions of fatty acids in the infant formulas vary between manufacturers and that the regio-specific distributions of the fatty acids on the glycerol backbone of the triacylglycerols in infant formulas were different from human and bovine milk.<sup>15–17</sup> Differences in chain lengths of the fatty acids in infant formulas could potentially result in varying degrees of the solubilization of drugs during lipolysis of triacylglycerols in the GI tract, depending on the physicochemical properties of the drug. We hypothesized that variations of the liberated fatty acid species from different infant formulas could alter the solubilization of OZ439 and FQ during digestion.

Therefore, this study investigated the solubilization behavior of OZ439 and FQ during the *in vitro* intestinal digestion of different infant formulas, with the aim of elucidating the effects of lipid compositions on drug solubilization. A schematic representation of this study is summarized in Figure 1. The importance of lipid chain lengths was confirmed using emulsions of simple TAGs of medium- and long-chain fatty acids. The influence of fat content on drug solubilization was also assessed. Synchrotron small-angle X-ray scattering (SAXS) was used in two ways. First, it was used to detect the presence of crystalline OZ439+FQ and the polymorphic forms of OZ439 during *in situ* lipolysis by tracking diffraction peaks at wider angles. Second, SAXS was also used to understand changes in lipid self-assembly during digestion by tracking scattering features at lower angles concurrently. Liquid chromatography coupled to mass spectrometry (LC-MS) was used to determine the lipid compositions of the infant formulas. High-performance liquid chromatography (HPLC) was used to quantify the distributions of OZ439 and FQ in the digested phases of the infant formulas.

## 2. EXPERIMENTAL SECTION

**2.1. Materials and Chemicals.** OZ439-mesylate salt was provided by the Medicines for Malaria Venture (MMV;

Geneva, Switzerland). Ferroquine granules (containing 50 wt % active pharmaceutical ingredient (API)) were supplied by Sanofi (Montpellier, France). Infant formula powders from three different suppliers (brands not disclosed as they are commercial-in-confidence) were generously provided by MMV. Bovine milk (Pauls brand, 3.8 wt % fat) was purchased from local supermarkets (Victoria, Australia). Nutritional information on milk and the infant formula powders was summarized in Table S1 in the Supporting Information. Reagent-grade trizma maleate, sodium taurodeoxycholate hydrate (NaTDC,  $\geq 95\%$  purity), sodium azide ( $\geq 99\%$  purity, Fluka), tricaprylin ( $\geq 90\%$  purity), caprylic acid ( $\geq 99\%$  purity), and 4-bromophenylboronic acid (4-BPBA) were purchased from Sigma-Aldrich (St. Louis, MO). Triolein ( $>80\%$  purity) was purchased from Tokyo Chemical Industry (Japan). Oleic acid ( $>99\%$  purity) was purchased from NuChekPrep (MN, US). Calcium chloride dihydrate ( $>99\%$  purity) and sodium hydroxide pellets ( $\geq 97\%$  purity) were purchased from Ajax Finechem (New South Wales, Australia). Hydrochloric acid (36% solution) was purchased from LabServ (Ireland). Sodium chloride ( $>99\%$  purity) was purchased from Chem Supply (South Australia, Australia). DOPC (1,2-Dioleoyl-*sn*-glycero-3-phosphocholine) was purchased from Cayman Chemical (MI, US). Trifluoroacetic acid (TFA,  $\geq 99.9\%$  purity) was purchased from VWR (HiPerSolv CHROMANORM for HPLC, Australia). Acetonitrile (liquid chromatography grade) and tetrahydrofuran (THF, ACS grade) were purchased from Merck (Darmstadt, Germany). Lipase (USP-grade pancreatin extract) was purchased from Southern Biologicals (Victoria, Australia). Medium-chain triacylglycerols of caprylic acid/capric acid (MCT; Labrafac lipophile WL 1349) was a gift from Gattefossé. Long-chain triacylglycerols rich in *sn*-2 palmitate (LCT; Infat CC) was a gift from Enzymotec Ltd. (Migdal Haemek, Israel). Milk fat globular membrane (MFGM)-enriched whey protein concentrate was kindly provided by Arla Foods Ingredients Group P/S (Viby J, Denmark). Unless otherwise stated, all chemicals were used as received without further purification. Water was sourced from a Millipore Milli-Q water purification system at the point of use.

**2.2. In Vitro Lipolysis of OZ439 and FQ in Infant Formulas.** *In vitro* lipolysis of the three infant formulas (IF 1, IF 2, and IF 3) at 20, 30, or 40 g of IF powders/200 mL of

digestion buffer (termed 20, 30, or 40 g equivalent, respectively) with and without OZ439-mesylate+FQ granules was performed using methods described previously.<sup>9</sup> The digestion buffer was 50 mM Tris-maleate at pH 6.5 that contained 150 mM NaCl, 5 mM CaCl<sub>2</sub>·2H<sub>2</sub>O, and 6 mM NaN<sub>3</sub>. OZ439 and FQ were dosed with equivalent free base (FB) amounts of 800 mg and 900 mg per 200 mL of IF solution, respectively. OZ439 has been previously administered to children following consumption of 200 mL of milk, but due to the limitations of the sample volume in the *in vitro* digestion apparatus, experiments were performed with smaller batches while the ratios of the drug to fat content in the IF were kept constant.

Briefly, 99 mg of OZ439-mesylate (equivalent to 82 mg OZ439-FB) and 186 mg of FQ granules (equivalent to 93 mg of FQ-FB) were added to 2.75 mL of water containing 0.25 mL of a 1 M HCl solution to simulate a gastric step, forming a OZ439-HCl salt.<sup>18</sup> IF powders, i.e., 2.03 g (20 g equivalent to total powder), 3.04 g (30 g equivalent to total powder), and 4.05 g (40 g equivalent to total powder) were prepared in 17.5 mL of a digestion buffer and were mixed with the acidic drug solution in a thermostat digestion vessel (37 °C) under constant magnetic stirring. Table 1 summarizes the amount of

**Table 1. Summary of the Fat Content (w/v %) and the Amount of OZ439-FB and FQ-FB (in mg of Drug/g of Fat) in Bovine Milk and Three Infant Formulas (IF 1, IF 2, and IF 3) during Digestion<sup>a</sup>**

gram equivalent of IF powder	fat content during digestion (%)			
	IF 1	IF 2	IF 3	bovine milk
20	2.5	2.7	2.6	3.3
30	3.8	4.1	3.9	
40	5.1	5.4	5.2	
gram equivalent of IF powder	mg of OZ439-FB/g of fat			
	IF 1	IF 2	IF 3	bovine milk
20	159.3	149.3	155.7	123.6
30	106.4	99.7	103.9	
40	79.9	74.9	78.0	
gram equivalent of IF powder	mg of FQ-FB/g of fat			
	IF 1	IF 2	IF 3	bovine milk
20	179.9	168.6	175.7	139.5
30	120.1	112.6	117.3	
40	90.2	84.5	88.1	

<sup>a</sup>Gram equivalents of the IF powders were representative of the amount of IF powder (20, 30, or 40 g) per 200 milliliters of digestion buffer.

dosed OZ439 and FQ per gram of fat in all the IFs at 20, 30, and 40 g equivalent (eq) samples. The pH of the drug/IF samples was adjusted to  $6.500 \pm 0.003$  prior to the injection of 2.25 mL of a porcine pancreatic lipase suspension (about 700 tributyrin units/mL digest). The pancreatic lipase was prepared from freeze-dried pancreatin extract using methods previously described.<sup>19</sup> The pH of the samples was maintained at 6.5 during digestion by the pH-STAT controller (Metrohm 902 STAT titration system) with automated dosing of 2 M NaOH.

**2.3. *In Vitro* Lipolysis of OZ439 and FQ in Medium- and Long-Chain Simple Triacylglycerol Emulsions.** Lipid dispersions of MCT and LCT were prepared in digestion buffer both in the absence or presence of bile salt/

phospholipid mixed micelles (4.7 mM NaTDC and 0.98 mM DOPC), as described previously.<sup>6</sup> Triacylglycerols (0.76 g) were added to a MFGM emulsifier (0.11 g) in 10 mL of digestion buffer, and the mixtures were sonicated with 2 s on/off cycles (25% amplitude) for 3 and 4 min processing times (Misonix S-4000 ultrasonic liquid processor, NY, US) for MCT and LCT, respectively. The volume of the samples was made up to 20 mL with the digestion buffer. OZ439-mesylate (99 mg) and FQ granules (186 mg) were added to 2.75 mL of water containing 0.25 mL of a 1 M HCl solution. The acidic drug mixtures were added to 17.5 mL of the emulsified MCT or LCT, and transferred to the 37 °C digestion vessel. *In vitro* lipolysis of the samples was performed as described in section 2.2. The fatty acids released from the lipid during digestion were titrated using 0.2 M (for LCT) or 2.0 M (for MCT) NaOH to maintain a pH of 6.5.

**2.4. Synchrotron Small-Angle X-ray Scattering: Lipid Self-Assembly and Solubilization of OZ439/FQ in the Infant Formulas during *In Vitro* Lipolysis.** The characterization of the liquid crystalline structures formed by self-assembly of the lipolytic products in the IFs and the solubilization of OZ439 and FQ were performed using the small and wide-angle X-ray scattering (SAXS/WAXS) beamline at the Australian Synchrotron (ANSTO, Clayton, Victoria, Australia). The pH-STAT apparatus was interfaced to SAXS, where samples were aspirated from the digestion vessel using a peristaltic pump to a fixed quartz capillary mounted in the X-ray beam (13 keV, wavelength of 0.954 Å) and circulated back into the vessel.<sup>20</sup> A sample-to-detector distance of approximately 1.6 m ( $0.01 < q < 0.40 \text{ \AA}^{-1}$ ) and 0.6 m ( $0.04 < q < 2.00 \text{ \AA}^{-1}$ ) was used to detect the liquid crystalline structures of the self-assembled lipids and the crystalline drug signals, respectively.  $q$  is the length of the scattering vector defined by  $4\pi/\lambda \sin(2\theta/2)$ ,  $2\theta$  is the scattering angle, and  $\lambda$  is the X-ray wavelength. 2D SAXS patterns were recorded using a Pilatus 1 M detector with a 5 s acquisition time and a 15 s measurement delay. The raw data were reduced to functions of  $I(q)$  versus  $q$  by radial integration using the in-house software ScatterBrain (Version 2.71).

**2.5. Analysis of the Lipid Compositions in Milk and Infant Formulas Using LC-MS.** Compositions of lipids in milk and IFs before and after 30 min of digestion were analyzed using LC-MS to identify key lipid components that dictate drug solubilization. Changes in the fatty acid and monoglyceride species in bovine milk, IF 1, and IF 2 during digestion have been recently reported.<sup>21</sup> *In vitro* lipolysis of milk, 40 g eq IF 1, IF 2, and IF 3 were performed using methods described in section 2.2. Samples (200  $\mu$ L) were collected after 30 min of digestion and added to 2  $\mu$ L of lipase inhibitor (0.5 M 4-BPBA in methanol). The extraction of lipids from the digested milk and IF was performed using methods described previously.<sup>21</sup> Briefly, samples were diluted with water and added to mixtures of chloroform:methanol (2:1 volume ratio) and 1-butanol/methanol (1:1 volume ratio) containing isotopically labeled fatty acid internal standards.<sup>21</sup> The samples were mixed and sonicated in an iced water bath for 30 min and left to equilibrate at room temperature for 20 min followed by centrifugation at  $16000 \times g$  for 10 min. The supernatant was transferred to a 96-deep-well plate and dried overnight under nitrogen gas flow. 1-Butanol (100  $\mu$ L) was added to the dried samples and sonicated for 10 min followed by the addition of methanol

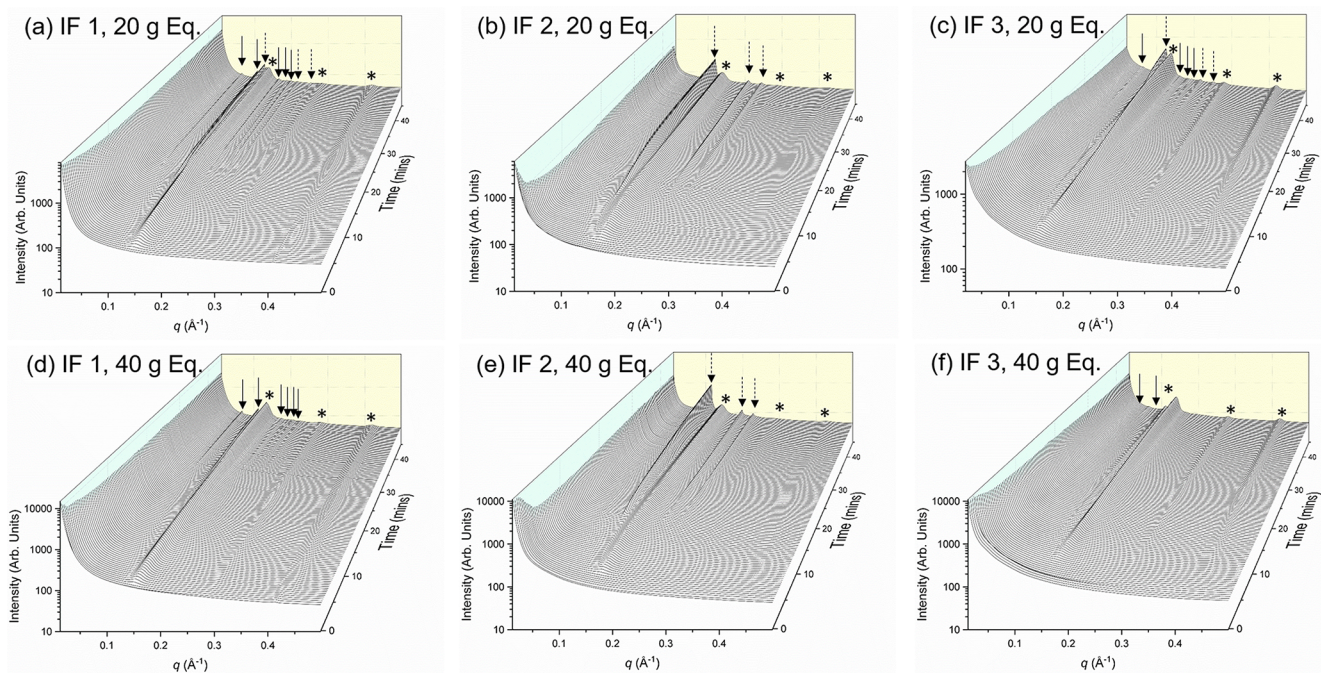


**Figure 2.** X-ray scattering patterns as a function of digestion time of the three infant formulas IF 1, IF 2 and IF 3 at low (20 g eq; panels a–c) and high (40 g eq; panels d–f) fat contents. The gram equivalents were representative of the amount of IF powder used for coadministration of 800 mg of OZ439-FB and 900 mg of FQ-FB in a total volume of 200 mL. Solid arrows represent peaks of the  $Fd3m$  phase, dashed arrows represent peaks for the  $H_2$  phase, and asterisks depict peaks of the  $L_{\alpha}$  phase from calcium soaps.

(100  $\mu\text{L}$ ) and centrifugation at  $3700 \times g$  for 5 min. The supernatants were transferred to glass vials and injected onto an LC (Shimadzu Nexera X2) coupled to a tandem triple quadrupole mass spectrometer (Shimadzu 8050) with an electrospray ionization (ESI) source operating at a negative ion mode. Reversed phase separation of the lipids in the digested milk and IFs was performed using a Waters Symmetry C18 column ( $4.6 \times 75 \text{ mm}^2$ ,  $3.5 \mu\text{m}$ ; Waters Symmetry) at  $40 \text{ }^\circ\text{C}$  on a binary phase gradient at  $0.4 \text{ mL/min}$  using water:acetonitrile (9:1 volume ratio) and acetonitrile:isopropanol (1:9 volume ratio) as solvent A and solvent B, respectively. The elution gradient consisted of a gradual increase of solvent B from 0 to 60% B (3 min), 60–92% B (8 min), 92% B (3.5 min), and 92–0% B (2 min).

**2.6. Distributions and Quantification of OZ439 and FQ in the Digested Infant Formulas Using HPLC.** Samples (200  $\mu\text{L}$ ) before (0 min) and after 30 min of digestion of OZ439 and FQ in infant formulas were collected, and 2  $\mu\text{L}$  of 4-BPBA (0.5 M in methanol) was added to inhibit digestion. The samples were ultracentrifuged at  $434900 \times g$  for 1 h at  $37 \text{ }^\circ\text{C}$  (Optima MAX-TL ultracentrifuge, Beckman Coulter, IN, US). The resultant phases (typically consisting of a dense pellet, a supernatant, and a buoyant lipid layer) were collected separately, and the drugs were extracted. Methanol (200  $\mu\text{L}$ ) and DMSO (800  $\mu\text{L}$ ) containing internal standards (diazepam) were added to the lipid and pellet layers prior to dilution with a mobile phase containing 95% solvent A (0.1% TFA in water) and 5% solvent B (0.085% TFA in acetonitrile). For the supernatant phase, 100  $\mu\text{L}$  of the aqueous sample was added to 100  $\mu\text{L}$  of methanol and 800  $\mu\text{L}$  of DMSO containing diazepam. Chromatographic separation of OZ439 and FQ was performed using a reverse-phase C18 column ( $4.6 \times 75 \text{ mm}^2$ ,  $3.5 \mu\text{m}$ ,  $100 \text{ \AA}$ ; Waters Symmetry) at  $35 \text{ }^\circ\text{C}$  with a UV detector (Shimadzu Corporation) on a

binary phase gradient that consisted of 5–95% B (6 min), 95% B (0.2 min), and 5% B (5.8 min). The flow rate was 0.5 mL/min, and the injection volume was 10  $\mu\text{L}$ .

**2.7. Solubility of OZ439 and FQ in Triglycerides and Fatty Acids.** Excess amounts of OZ439-FB 2 (prepared using methods in ref 18) and FQ-API were weighed into triolein, tricaprylin, oleic acid, and caprylic acid. Samples were incubated at  $37 \text{ }^\circ\text{C}$  on a rotary shaker, and aliquots were removed after 4 h, 1 d, and 4 d of incubation followed by ultracentrifugation at 278 and  $300 \times g$  for 30 min at  $37 \text{ }^\circ\text{C}$  (Optima MAX-TL ultracentrifuge, Beckman Coulter, IN, US). The supernatant was removed and stored at  $-20 \text{ }^\circ\text{C}$  prior to drug quantification using HPLC. Mixtures of 1:1 v/v THF:acetonitrile were added to the supernatant, and samples were diluted in the mobile phase described in section 2.6. The equilibrium solubility was the solubility value that differed less than 10% between the time points. Measurements were performed in triplicate.

**2.8. Particle Size Measurements.** Volume-based size distributions of the lipid emulsions in infant formula, MCT, and LCT were measured using a Mastersizer S (Malvern Panalytical, Worcestershire, UK) equipped with a He–Ne laser (wavelength 633 nm) and a 300-RF lens to detect particle sizes between 0.05 and 880  $\mu\text{m}$ . The sample was added to 50 mL of water to achieve an obscuration rate between 10 and 15. The particle density of the lipid was taken to be  $0.92 \text{ g/cm}^3$ , and the refractive index of the lipid was 1.46 and that for water was 1.33. Particle sizes were reported as the volume mean  $D_{4,3}$ , defined as  $\sum n_i d_i^4 / \sum n_i d_i^3$ , where  $n_i$  is the number of particles with diameter  $d_i$ .

### 3. RESULTS AND DISCUSSION

#### 3.1. Formation of Liquid Crystalline Structures during Digestion in the Absence and Presence of

**OZ439 and FQ.** Previous studies have shown that variations in the lipid species in milk and infant formula are key to the formation of different liquid crystalline structures during digestion,<sup>21</sup> which may subsequently impact the delivery of nutrients and coadministered drugs. Herein, the self-assembly of lipids during digestion of three infant formulas was determined, and the impacts of OZ439 and FQ on the colloidal structures formed were investigated.

Formation of lipid structures via the self-assembly of the lipolytic products in the IFs during *in vitro* lipolysis is shown by the SAXS data in Figure 2. Digestion of IF1, IF2, and IF3 produced different liquid crystalline structures compared to bovine milk due to the different MAG and FFA species liberated. The amount of MAGs and FFAs species released after 30 min of digestion is summarized in Table S2. IF 2 contained more medium-chain fatty acids compared to IF 1 and IF 3, which explained the formation of an inverse hexagonal phase ( $H_2$ ) during digestion as opposed to IF 1 and IF 3, where the formation of an inverse micellar cubic phase  $Fd3m$  was promoted due to the higher negative curvature of the lipids. These structures were not affected by the total amount of lipids explored in our studies (Figure 2; 20 g vs 40 g eq); however, a delayed formation of the liquid crystalline structures in higher fat infant formulas could be seen, which could be attributed to the slower lipolysis (see Figure S1 for the titration profiles). This observation agrees well with previous a study<sup>22</sup> and may be correlated to the decrease in the ratio of lipase to fat globules, the ratio of calcium to FFA that aids the removal of FFA from the surface of the fat globules, and the aggregation of the fat globules at high fat contents. Measurements of the size distributions of the fat globules in IF 2 at 2.7% fat (20 g eq) and 5.4% fat (40 g eq) showed that the volume mean diameters ( $D_{4,3}$ ) were 0.83 and 2.12  $\mu\text{m}$ , respectively. Size distribution profiles of the fat globules are given in Figure S2.

The addition of OZ439 and FQ into all of the infant formulas prior to digestion was found to disrupt the formation of the colloidal structures irrespective of the initial liquid crystalline phases (Figure 3). A similar behavior has been observed in milk; however, the effects of drugs on the self-assembled structures were dependent on the amount of

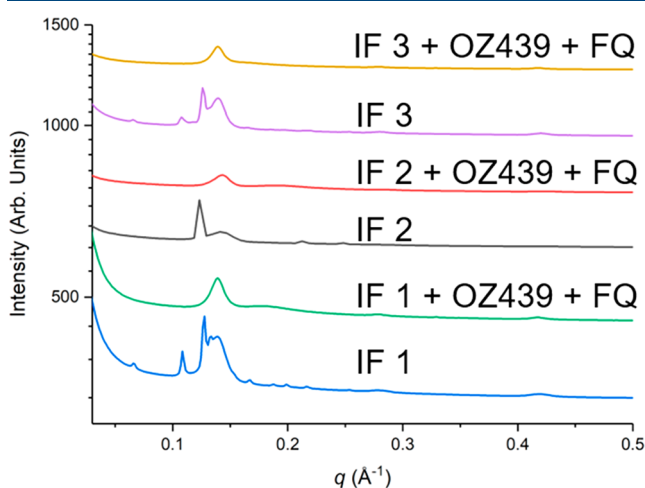


**Figure 3.** Comparisons in the X-ray scattering patterns between infant formulas and infant formulas containing OZ439 and FQ after 30 min of digestion.

coadministered OZ439 and FQ, with FQ exerting a stronger effect on the structures compared to OZ439.<sup>9</sup> This may be caused by greater interactions between FQ and the milk lipids generally, but it is unknown whether preferential binding between the different types of FFA and the drug species occurred. We therefore anticipated that any differences observed in the extent of drug solubilization during digestion in the three infant formulas would be due to the types of lipolytic products released and not the structural effects of the colloidal phases.

**3.2. Solubilization of OZ439 and FQ in Infant Formulas and the Effects of Fat Content: SAXS and HPLC Studies.** The solubilization of OZ439 and FQ in IF 1, IF 2, and IF 3 during dispersion and digestion was determined using SAXS. This technique has been previously shown to be useful in the simultaneous monitoring of both the kinetics of the solubilization and the polymorphic phase transformation of drugs in real time.<sup>6,8,9,23,24</sup> The scattering of X-rays by the crystalline drugs gives rise to sharp Bragg peaks; and the decrease in the peak areas, i.e., the loss of crystallinity, can be interpreted as solubilization or amorphization.

It is known that OZ439 undergoes a polymorphic transformation from the crystalline free-base form 1 (OZ439-FB 1) at the small intestinal pH to the stable form 2 polymorph (OZ439-FB 2) during storage<sup>18</sup> or digestion in milk,<sup>8</sup> and a similar behavior was seen in the digesting infant formulas. The evolution of OZ439-FB 2 with the digestion time is shown in Figure S3. A comparison between the solubilization of OZ439 in milk and IFs was therefore assessed based on the final scattering intensity from OZ439-FB 2 crystals present after digestion. Figure 4a shows that the final extent of formation of the OZ439-FB 2 crystals (that could potentially dictate oral bioavailability) differed across the IFs. For 20 g eq powders, less OZ439-FB2 was formed after 30 min of digestion of IF 2 compared to IF 1 and IF 3. We also observed that the amount of OZ439-FB 2 crystals remaining in the sample was dependent on the fat content of the infant formulas, with 40 g eq IF 2 providing a near-complete disappearance of the characteristic Bragg peak at  $q = 1.27 \text{ \AA}^{-1}$ . The influence of the fat content on the drug solubilization has also been shown in milk, utilizing halofantrine as a model weakly basic drug.<sup>7</sup>

The degree of solubilization of OZ439 in all of the infant formulas was different, with the performance ranking as follows: IF 2 > IF 1 > IF 3. An examination of the key differences in the lipid components between the three infant formulas using LC-MS revealed that IF 2 contained a higher amount of C8:0–C12:0 medium-chain lipids (FFAs and MAGs) after 30 min of digestion, with mole ratios of approximately 1/3.3/1.2 in IF 1/IF 2/IF 3, respectively (Table S2). The greater number of moles of lipids in IF 2 could therefore support the solubilization of OZ439, as evidenced from the total amount of released fatty acids during *in vitro* digestion (Figure S4).

In addition, the solubilization of OZ439-FB 2 was found to be affected by the kinetics of the release of fatty acids during *in vitro* digestion. In IF 3, for example, more undissolved OZ439-FB 2, i.e., a larger peak area of the characteristic Bragg peak, was observed after digestion that could be caused by the slower release of fatty acids (Figure S4). Preliminary investigations of the total phospholipid contents in the infant formulas using LC-MS show a higher relative amount of lysophosphatidylethanolamine in IF 3 compared to IF 1 and

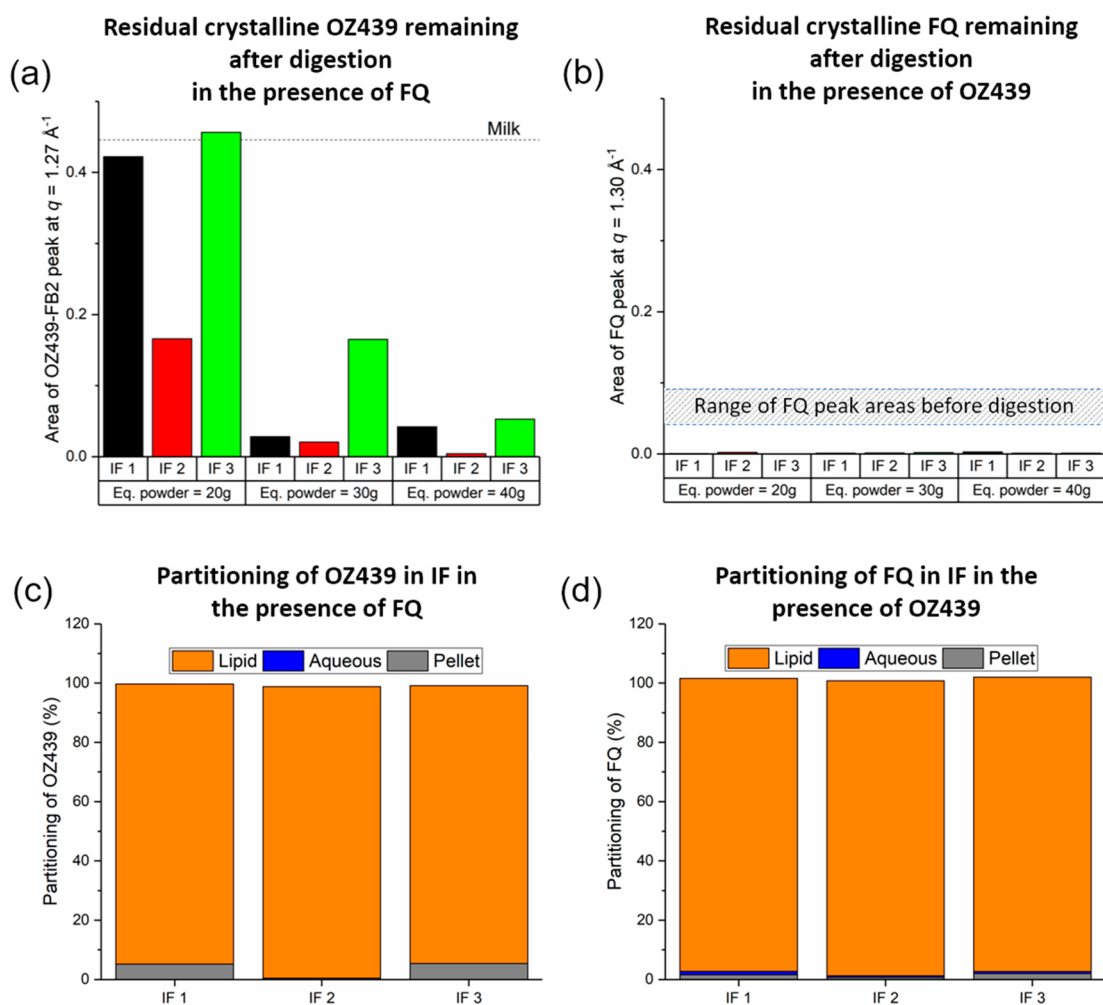


**Figure 4.** Residual crystalline (a) OZ439-FB 2 and (b) FQ remaining after 30 min of digestion in infant formulas IF 1, IF 2, and IF 3 from 20 g eq powders (2.5–2.7% fat) to 40 g eq powders (5.1–5.4% fat). Residual peak area of OZ439-FB 2 after 30 min of digestion of milk (3.3% fat) was also shown for comparison (dashed line). Partitioning of OZ439 and FQ in the digested phases of the infant formulas at 40 g eq powders collected after 30 min of digestion is shown in panel c and d, respectively.

IF 2, suggesting that the presence of excipients in infant formulas can affect the degree of drug solubilization due to their impact on the kinetics of lipid digestion.

Unlike OZ439, where the formation of OZ439-FB 2 during digestion was dependent on the type of infant formula and the release of fatty acids, the disappearance of the crystalline FQ Bragg peak during digestion was not significantly affected by the type of infant formula. Figure 4b shows the area under the characteristic Bragg peak for FQ at  $q = 1.30 \text{ \AA}^{-1}$  in IF 1, IF 2, and IF 3 from 20 to 40 g eq powders after 30 min of digestion. The disappearance of the FQ peak was observed in all tested samples. The loss of crystallinity in FQ during digestion in the infant formulas was therefore postulated to be independent of the type of lipid species and the amount of fat when  $\geq 2.5\%$  fat content was used. Separate investigations into the threshold concentrations of fat onto which FQ could be solubilized in IF 2 (Figure S5) showed the presence of FQ crystals when the fat content was between  $\sim 5 \text{ g eq}$  and  $10 \text{ g eq}$  IF 2 powder. The solubilization of FQ could therefore be achieved with an IF 2 fat content between 0.7% (5 g eq) and 1.4% (10 g eq), as was shown in Figure S5. Although OZ439 and FQ have similar values of  $\log P$ , their  $pK_a$  values are different (Figure 1). At pH 6.5 during digestion, ferroquine

exhibits a greater degree of ionization compared to OZ439, which was hypothesized to enable a greater interaction between the protonated form of ferroquine and the liberated ionized fatty acids. It has been shown previously that where ferroquine reduced the solubilization of OZ439 during the digestion of milk due to competition for the available fatty acids.<sup>9</sup>

Comparative solubilization studies of OZ439 and FQ in the three infant formulas during digestion were subsequently performed using HPLC, and the amount of drug partitioned into the dense pellet, the supernatant, and the buoyant lipid phases was quantified. Insignificant amounts of FQ were observed in the pellet phase, indicating essentially complete drug solubilization (Figure 4d); while the amount of OZ439 remaining in the pellet phase after digestion in IF 2 was lower than in IF 1 and IF 3 (Figure 4c). The higher extent of drug solubilization could therefore be attained in medium-chain FA-rich IF 2, which agrees well with the observations from SAXS described previously.

To elucidate whether the differences in the chain lengths of FA species would affect the degree of drug solubilization, the saturation solubility of OZ439 and FQ in medium- and long-chain FAs was determined using caprylic acid and oleic acid as

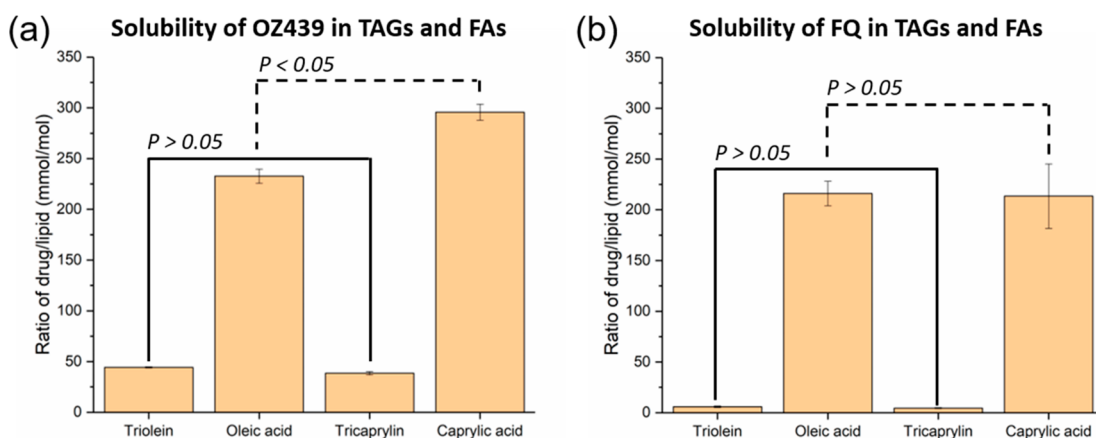


**Figure 5.** Equilibrium solubility of (a) OZ439-FB 2 and (b) FQ-FB in triacylglycerols (triolein and tricaprylin) and fatty acids (oleic acid and caprylic acid) in units of mmol of drug/mol of lipid.

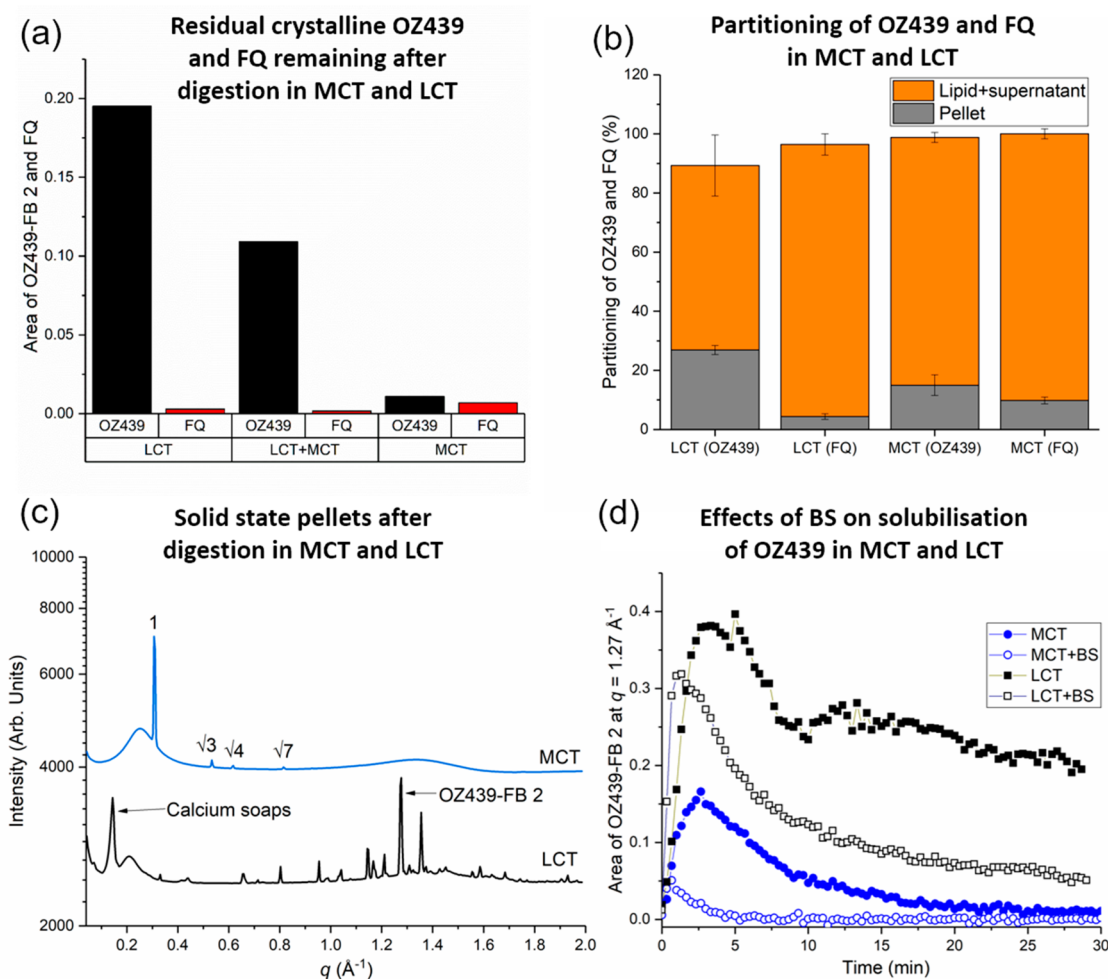


**Figure 6.** (a) Residual crystalline OZ439-FB 2 (characteristic peak at  $q = 1.27 \text{ \AA}^{-1}$ ) and FQ (characteristic peak at  $q = 1.30 \text{ \AA}^{-1}$ ) remaining after 30 min of digestion of MCT and LCT emulsions. (b) Partitioning of OZ439 in MCT and LCT after 30 min of digestion. (c) The X-ray scattering patterns of the resulting pellets. Peaks in the low  $q$  region in the pellet of the digested MCT sample were indexed to a hexagonal liquid crystal phase with spacing ratios of  $1:\sqrt{3}:\sqrt{4}:\sqrt{7}$ . (d) Effects of bile salts on the solubilization of OZ439 during the course of digestion.

the model lipids, respectively. The solubility of drugs in the corresponding TAGs, i.e., tricaprylin and triolein, was also assessed to determine the differential solubility values of OZ439 and FQ between TAGs and FAs. Compounds that

exhibited greater solubility differences between FAs and the corresponding TAGs were hypothesized to give rise to a higher drug solubilization after digestion where FA was released.

Figure 5 shows the higher solubility of OZ439-FB 2 (the most stable polymorph) in medium-chain fatty acids compared to long-chain fatty acids, but no significant difference was observed in the solubility of OZ439 in the TAGs. Therefore, the enhanced solubilization of OZ439 in IF 2 could be driven not only by the greater amount of fat present per weight of powder but also by the higher solubility of the drug in medium-chain fatty acids, which constitute a greater proportion of IF 2. No significant impact of fatty acid chain lengths on the solubility of FQ could be detected.

Meanwhile, greater amounts of OZ439 and FQ could be solubilized in FAs compared to TAGs on a mmol/mol basis irrespective of the fatty acid chain lengths, and larger solubility differences (between TAGs and FAs) were observed for FQ compared to OZ439. About a 36-fold increase in the drug solubility was attained for FQ compared to only a ~5-fold increase for OZ439 in long-chain lipids. For medium-chain lipids, solubility increases of ~46-fold and 7-fold were observed for FQ and OZ439, respectively. Larger solubility differences between TAGs and FAs for FQ will therefore lead to a greater extent of drug solubilization when fatty acids are released during digestion compared to OZ439. The solubility of OZ439-FB 2 and FQ on an equivalent mass basis (mg of drug/g of lipid) is presented in Figure S6.

**3.3. Solubilization of OZ439 and FQ in Simple Triacylglycerol Emulsions and the Effects of Bile Salts.** To confirm the hypothesis that the greater solubilization of OZ439 in IF 2 was due to the presence of more medium-chain lipids, the solubilization of OZ439 and FQ in emulsified MCT and LCT was investigated using SAXS. Generally, lipid-based formulations containing MCT have a tendency to provide greater initial solubilization of drugs; however, the digested products may have a reduced capacity to support drug solubilization compared to LCT due to the higher polarity of the FA.<sup>25,26</sup> The use of MCT as an oral-based lipid formulation has therefore been reported to favor the solubilization of less lipophilic drugs<sup>27</sup> and not highly lipophilic compounds due to drug precipitation during *in vitro* digestion.<sup>28</sup> However, it is worth noting that the formation of drug-rich pellet phases may not necessarily translate to a reduced oral bioavailability, particularly when amorphous solids with high dissolution rates are formed.<sup>29,30</sup>

OZ439 and FQ are weakly basic lipophilic drugs that have log *P* values of about 5.4 and 5.1, respectively, and may therefore exhibit a lower extent of solubilization in MCT during *in vitro* digestion. Comparisons between the area under the characteristic OZ439-FB 2 peak at  $q = 1.27 \text{ \AA}^{-1}$  in Figure 6a, however, showed the presence of fewer OZ439-FB 2 crystals in MCT than LCT after digestion, indicating that the lipolytic products of the medium-chain TAGs played an important role in the solubilization of OZ439. Fewer OZ439-FB 2 drug crystals were also observed when 20 wt % of the fat in LCT was substituted with MCT, further suggesting that the inclusion of MCT may be considered as a beneficial approach to improve the solubilization of OZ439 and that less lipid (on a weight basis) would be required to achieve a similar level of drug solubilization.

The quantification of the amount of OZ439 and FQ partitioned into the digested phases of MCT and LCT after ultracentrifugation using HPLC is shown in Figure 6c. Ultracentrifugation of the digested phases of OZ439+FQ in LCT resulted in a dense pellet, a clear supernatant phase, and a lipid phase, while, in MCT, the separated layers consisted of

a clear supernatant phase and two sedimented phases (that consisted of a “solid” yellow pellet layer and an “oily” yellow drug-rich phase) where most of OZ439 and FQ reside (Figure S7). An analysis of the “solid” pellet layer in the digested MCT using HPLC showed the presence of about 15% OZ439 and 10% FQ, while >80% OZ439 and 90% FQ was partitioned into the sedimented “oily” layer and the supernatant (Figure 6b). It is worth noting that the amount of drug partitioned in the “lipid and supernatant” layers presented in Figure 6b was a summation of the drugs residing in the sedimented “oily” layer and the aqueous supernatant layer due to difficulties of phase separation. A solid-state analysis of the collected pellets in MCT using SAXS (Figure 6c) showed the presence of a broad halo characteristic of random molecular distributions, with no periodic crystal lattice planes and with no observable Bragg peaks characteristic of crystalline OZ439-FB 2 and FQ. Meanwhile, sharp Bragg peaks indicative of OZ439-FB 2 crystals could be seen in the pellet of the digested LCT samples. Our results therefore suggest that OZ439 precipitated mainly in an amorphous form during digestion in MCT, which may subsequently redissolve more rapidly in an intestinal environment and thereby increase the flux of drug across the intestinal membrane.<sup>31,29,30</sup>

Similar trends in the solubilization of OZ439 could be observed with the inclusion of bile salt micelles (NaTDC/DOPC) during the digestion of MCT and LCT; however, the extent of solubilization was influenced by the presence of these endogenous surfactants. Figure 6d shows that the presence of bile salt micelles provided significant improvements in the solubilization of OZ439-FB 2 in LCT, and fewer drug crystals were also observed in the MCT-based lipid formulations after digestion. This suggested a potential solubilization of OZ439 into the mixed micelles formed by the incorporation of FFA and MAG into NaTDC/DOPC<sup>32</sup> during digestion.<sup>33,34</sup> It should also be noted that an overall increase in the amount of titrated NaOH, and hence the released fatty acids, during the lipolysis of lipids with drugs and bile salts (see Table S3) may also contribute to the improved solubilization of OZ439. This increase could be caused by the enhanced removal of the lipolytic products that accumulated at the oil–water interface of the fat globules,<sup>35,36</sup> which subsequently increased the exposure of the TAG core to pancreatic lipases. The characterization of the particle size distributions of the fat globules showed that the presence of bile salts may also assist in the emulsification of the lipids due to their amphiphilic nature,<sup>2</sup> leading to smaller-sized fat globules with narrower size distributions (Figure S8).

In addition to the overall enhanced solubilization of OZ439 during digestion in MCT and LCT, the addition of bile salts affected the kinetics of the formation of OZ439-FB 2 (see Figure 6d), which may be caused by changes in the supersaturation state of the drug. We have previously shown that the precipitation of OZ439-FB 2 (in the absence of FQ) occurred during digestion and not dispersion, and this could be attributed to the nucleation and growth of OZ439-FB 2 crystals from the thermodynamically unstable supersaturated state of OZ439-FB.<sup>8</sup> The supersaturated solution arises when the solubilization capacity of OZ439 decreases during lipolysis as the colloidal species become progressively more hydrophilic. Hence, a supersaturated drug solution may also be achieved when FFA is solubilized into the NaTDC/DOPC mixed micelles, thereby depleting the FFA species available for



drug solubilization. This may in turn lead to faster kinetics of precipitation of OZ439-FB 2 in MCT and LCT, as was seen in Figure 6d.

Overall, our studies confirmed, based on the *in vitro* data, that medium-chain triacylglycerols (MCT) provide higher drug solubilization during digestion than long-chain triacylglycerols (LCT). Although MCT has been categorized as a “Generally Recognized as Safe” (GRAS) class of compound by the FDA<sup>37</sup> and its use as a substitute for LCT has been established (due to the faster digestion and absorption that can provide an immediate source of energy for infants with malabsorption issues and in prematurely born neonates),<sup>38,39</sup> the consumption of infant formulas containing high amounts of MCT for a long period of time is not recommended given the possible risk of deficiencies in fat-soluble nutrients.<sup>38</sup> Infant formulas containing mixtures of LCT and MCT may therefore provide beneficial effects in improving the oral bioavailability of OZ439 and promote growth in children.

#### 4. CONCLUSIONS

Understanding the correlation between drug solubilization and lipid compositions is key to the design of milk-based lipid formulations for the coadministration of drugs. In this study, the solubilization of the antimalarial drugs OZ439 and FQ in three infant formulas that have different lipid compositions was assessed. We conclude that infant formulas can be used as substitutes to milk as an oral-based formulation to deliver OZ439 and FQ, with lipid compositions being the key parameters in dictating the solubilization of OZ439 and FQ. This study provides useful guidance in the design of simple LBF for the oral delivery of OZ439 and FQ and in the preliminary assessment of drug solubilization behaviors following administration to breast-fed infants.

#### ■ ASSOCIATED CONTENT

##### SI Supporting Information

The Supporting Information is available free of charge at <https://pubs.acs.org/doi/10.1021/acs.molpharmaceut.0c00475>.

Compositions of free fatty acids and monoacylglycerols in milk and infant formulas after 30 min of digestion; titrated fatty acids during the digestion of infant formulas; particle size distributions of IF 2 at 20 and 40 g eq powders; evolution of OZ439-FB2 during the digestion of infant formulas; total amount of titrated NaOH during the digestion of infant formulas; X-ray scattering profiles of OZ439+FQ in IF 2 at variable fat contents; equilibrium solubility of OZ439-FB2 and FQ-FB in triacylglycerols and fatty acids; visual observations of the separated digested phases of OZ439 and FQ in MCT and LCT; particle size distributions of milk, MCT, and LCT dispersions in the absence and presence of bile salts; and amount of titrated fatty acids liberated from MCT and LCT during digestion with and without bile salts (PDF)

#### ■ AUTHOR INFORMATION

##### Corresponding Author

**Ben J. Boyd** – *Drug Delivery, Disposition and Dynamics, Monash Institute of Pharmaceutical Sciences, Monash University, Parkville, Victoria 3052, Australia; ARC Centre of Excellence in Convergent Bio-Nano Science and Technology,*

*Monash Institute of Pharmaceutical Sciences, Monash University (Parkville Campus), Parkville, Victoria 3052, Australia; [orcid.org/0000-0001-5434-590X](https://orcid.org/0000-0001-5434-590X); Phone: +61 3 99039112; Email: [ben.boyd@monash.edu](mailto:ben.boyd@monash.edu); Fax: +61 3 99039583*

#### Authors

**Malinda Salim** – *Drug Delivery, Disposition and Dynamics, Monash Institute of Pharmaceutical Sciences, Monash University, Parkville, Victoria 3052, Australia; [orcid.org/0000-0003-1773-5401](https://orcid.org/0000-0003-1773-5401)*

**Gisela Ramirez** – *Drug Delivery, Disposition and Dynamics, Monash Institute of Pharmaceutical Sciences, Monash University, Parkville, Victoria 3052, Australia*

**Kang-Yu Peng** – *Drug Delivery, Disposition and Dynamics, Monash Institute of Pharmaceutical Sciences, Monash University, Parkville, Victoria 3052, Australia*

**Andrew J. Clulow** – *Drug Delivery, Disposition and Dynamics, Monash Institute of Pharmaceutical Sciences, Monash University, Parkville, Victoria 3052, Australia; [orcid.org/0000-0003-2037-853X](https://orcid.org/0000-0003-2037-853X)*

**Adrian Hawley** – *SAXS/WAXS beamline, Australian Synchrotron, ANSTO, Clayton, Victoria 3169, Australia*

**Hanu Ramachandruni** – *Medicines for Malaria Venture, Geneva 1215, Switzerland*

**Stephane Beilles** – *Sanofi R&D, Montpellier 34080, France*

Complete contact information is available at:

<https://pubs.acs.org/doi/10.1021/acs.molpharmaceut.0c00475>

#### Notes

The authors declare no competing financial interest.

#### ■ ACKNOWLEDGMENTS

This work was funded by the Bill and Melinda Gates Foundation under Investment ID OPP1160404 in collaboration with the Medicines for Malaria Venture (MMV). Funding is also acknowledged from the Australian Research Council under the Discovery Projects scheme DP160102906, and A.J.C. is the recipient of a discovery early career research award (DE190100531). The SAXS experiments for this work were conducted on the SAXS/WAXS beamline of the Australian Synchrotron, part of ANSTO. The authors thank Arla Foods Ingredients Group P/S for the donation of MFGM. We thank Dr. Niya Bowers, Dr. Michael Mitchell, and Dr. Drazen Ostovic for technical and historical discussions around the coadministration of OZ439 with infant formulas.

#### ■ ABBREVIATIONS

FQ, ferroquine; FB, free base; IF, infant formula; MCT, medium-chain triacylglycerols; LCT, long-chain triacylglycerols; TAG, triacylglycerols; MAG, monoacylglycerols; FA, fatty acids; BS, bile salts; SAXS, small-angle X-ray scattering; HPLC, high-performance liquid chromatography; LBF, lipid-based formulations; MFGM, milk fat globular membrane

#### ■ REFERENCES

(1) Porter, C. J. H.; Charman, W. N. Oral lipid-based formulations: using preclinical data to dictate formulation strategies for poorly water-soluble drugs. In *Oral lipid-based formulations: enhancing the bioavailability of poorly water-soluble drugs*; Hauss, D. J., Ed.; CRC Press, 2007; Vol. 170, p 185.

- (2) Carey, M C; Small, D M; Bliss, C M Lipid Digestion and Absorption. *Annu. Rev. Physiol.* **1983**, *45* (1), 651–677.
- (3) Patton, S. Origin of the milk fat globule. *J. Am. Oil Chem. Soc.* **1973**, *50* (6), 178–185.
- (4) Clulow, A. J.; Salim, M.; Hawley, A.; Boyd, B. J. A closer look at the behaviour of milk lipids during digestion. *Chem. Phys. Lipids* **2018**, *211*, 107.
- (5) Salentinig, S.; Phan, S.; Khan, J.; Hawley, A.; Boyd, B. J. Formation of Highly Organized Nanostructures during the Digestion of Milk. *ACS Nano* **2013**, *7* (12), 10904–10911.
- (6) Salim, M.; Ramirez, G.; Clulow, A. J.; Zhang, Y.; Ristorph, K. D.; Feng, J.; McManus, S. A.; Hawley, A.; Prud'homme, R. K.; Boyd, B. J. Solid-State Behavior and Solubilization of Flash Nano-precipitated Clofazimine Particles during the Dispersion and Digestion of Milk-Based Formulations. *Mol. Pharmaceutics* **2019**, *16*, 2755.
- (7) Boyd, B. J.; Salim, M.; Clulow, A. J.; Ramirez, G.; Pham, A. C.; Hawley, A. The impact of digestion is essential to the understanding of milk as a drug delivery system for poorly water soluble drugs. *J. Controlled Release* **2018**, *292*, 13–17.
- (8) Salim, M.; Khan, J.; Ramirez, G.; Clulow, A. J.; Hawley, A.; Ramachandruni, H.; Boyd, B. J. Interactions of artefenomel (OZ439) with milk during digestion: insights into digestion-driven solubilization and polymorphic transformations. *Mol. Pharmaceutics* **2018**, *15* (8), 3535–3544.
- (9) Salim, M.; Khan, J.; Ramirez, G.; Murshed, M.; Clulow, A. J.; Hawley, A.; Ramachandruni, H.; Beilles, S.; Boyd, B. J. Impact of Ferroquine on the Solubilization of Artefenomel (OZ439) during in Vitro Lipolysis in Milk and Implications for Oral Combination Therapy for Malaria. *Mol. Pharmaceutics* **2019**, *16* (4), 1658–1668.
- (10) Phyto, A. P.; Jittamala, P.; Nosten, F. H.; Pukrittayakamee, S.; Imwong, M.; White, N. J.; Duparc, S.; Macintyre, F.; Baker, M.; Möhrle, J. J. Antimalarial activity of artefenomel (OZ439), a novel synthetic antimalarial endoperoxide, in patients with *Plasmodium falciparum* and *Plasmodium vivax* malaria: an open-label phase 2 trial. *Lancet Infect. Dis.* **2016**, *16* (1), 61–69.
- (11) Medicines for Malaria Venture; Richmond Pharmacology Ltd. A Dose-escalation Study to Investigate Safety and Tolerability of OZ439. <https://clinicaltrials.gov/ct2/show/study/NCT01713608>.
- (12) Medicines for Malaria Venture; Richmond Pharmacology Ltd. Healthy Volunteer Study of the Pharmacokinetics of Oral Pipleraquine With OZ439 + TPGS Formulation in the Fasted State. <https://clinicaltrials.gov/ct2/show/study/NCT01853475?sect=X01256>.
- (13) Singh Kamal, S.; Kaur, D.; Singh, S.; Sharma, A.; Katual, M. K.; Kumar Garg, A.; Kumar, R. An Investigative and Explanatory Review on Use of Milk as a Broad-Spectrum Drug Carrier for Improvement of Bioavailability and Patient Compliance. *J. Young Pharm.* **2016**, *8* (2), 72.
- (14) FDA. Use of Liquids and/or Soft Foods as Vehicles for Drug Administration: General Considerations for Selection and In Vitro Methods for Product Quality Assessments. <https://www.fda.gov/regulatory-information/search-fda-guidance-documents/use-liquids-and-or-soft-foods-vehicles-drug-administration-general-considerations-selection-and-vitro>.
- (15) Straarup, E. M.; Lauritzen, L.; Faerk, J.; Høy, C.-E.; Michaelsen, K. F. The stereospecific triacylglycerol structures and Fatty Acid profiles of human milk and infant formulas. *J. Pediatr. Gastroenterol. Nutr.* **2006**, *42* (3), 293–9.
- (16) Lopez-Lopez, A.; Lopez-Sabater, M. C.; Campoy-Folgozo, C.; Rivero-Urgell, M.; Castellote-Bargallo, A. I. Fatty acid and sn-2 fatty acid composition in human milk from Granada (Spain) and in infant formulas. *Eur. J. Clin. Nutr.* **2002**, *56* (12), 1242–54.
- (17) Bar-Yoseph, F.; Lifshitz, Y.; Cohen, T. Review of sn-2 palmitate oil implications for infant health. *Prostaglandins, Leukotrienes Essent. Fatty Acids* **2013**, *89* (4), 139–143.
- (18) Clulow, A. J.; Salim, M.; Hawley, A.; Gilbert, E. P.; Boyd, B. The curious case of the OZ439 mesylate salt - an amphiphilic antimalarial drug with diverse solution and solid state structures. *Mol. Pharmaceutics* **2018**, *15* (5), 2027–2035.
- (19) Khan, J.; Rades, T.; Boyd, B. J. Lipid-Based Formulations Can Enable the Model Poorly Water-Soluble Weakly Basic Drug Cinnarizine To Precipitate in an Amorphous-Salt Form During In Vitro Digestion. *Mol. Pharmaceutics* **2016**, *13* (11), 3783–3793.
- (20) Khan, J.; Hawley, A.; Rades, T.; Boyd, B. J. In Situ Lipolysis and Synchrotron Small-Angle X-ray Scattering for the Direct Determination of the Precipitation and Solid-State Form of a Poorly Water-Soluble Drug During Digestion of a Lipid-Based Formulation. *J. Pharm. Sci.* **2016**, *105*, 2631–2639.
- (21) Pham, A. C.; Peng, K.-Y.; Salim, M.; Ramirez, G.; Hawley, A.; Clulow, A. J.; Boyd, B. J. Correlating Digestion-Driven Self-Assembly in Milk and Infant Formulas with Changes in Lipid Composition. *ACS Appl. Bio. Mater.* **2020**, *3* (5), 3087–3098.
- (22) Li, Y.; Hu, M.; McClements, D. J. Factors affecting lipase digestibility of emulsified lipids using an in vitro digestion model: Proposal for a standardised pH-stat method. *Food Chem.* **2011**, *126* (2), 498–505.
- (23) Boetker, J.; Rades, T.; Rantanen, J.; Hawley, A.; Boyd, B. J. Structural Elucidation of Rapid Solution-Mediated Phase Transitions in Pharmaceutical Solids Using in Situ Synchrotron SAXS/WAXS. *Mol. Pharmaceutics* **2012**, *9* (9), 2787–2791.
- (24) Boetker, J. P.; Rantanen, J.; Arnfast, L.; Doreth, M.; Rajjada, D.; Loebmann, K.; Madsen, C.; Khan, J.; Rades, T.; Mullertz, A.; Hawley, A.; Thomas, D.; Boyd, B. J. Anhydrate to hydrate solid-state transformations of carbamazepine and nitrofurantoin in biorelevant media studied in situ using time-resolved synchrotron X-ray diffraction. *Eur. J. Pharm. Biopharm.* **2016**, *100*, 119–27.
- (25) Kaukonen, A. M.; Boyd, B. J.; Charman, W. N.; Porter, C. J. Drug solubilization behavior during in vitro digestion of suspension formulations of poorly water-soluble drugs in triglyceride lipids. *Pharm. Res.* **2004**, *21* (2), 254–60.
- (26) Porter, C. J.; Kaukonen, A. M.; Taillardat-Bertschinger, A.; Boyd, B. J.; O'Connor, J. M.; Edwards, G. A.; Charman, W. N. Use of in vitro lipid digestion data to explain the in vivo performance of triglyceride-based oral lipid formulations of poorly water-soluble drugs: studies with halofantrine. *J. Pharm. Sci.* **2004**, *93* (5), 1110–21.
- (27) Grove, M.; Pedersen, G. P.; Nielsen, J. L.; Mullertz, A. Bioavailability of seocalcitol I: Relating solubility in biorelevant media with oral bioavailability in rats—effect of medium and long chain triglycerides. *J. Pharm. Sci.* **2005**, *94* (8), 1830–8.
- (28) Porter, C. J. H.; Kaukonen, A. M.; Boyd, B. J.; Edwards, G. A.; Charman, W. N. Susceptibility to Lipase-Mediated Digestion Reduces the Oral Bioavailability of Danazol After Administration as a Medium-Chain Lipid-Based Microemulsion Formulation. *Pharm. Res.* **2004**, *21* (8), 1405–1412.
- (29) Larsen, A. T.; Ohlsson, A. G.; Polentarutti, B.; Barker, R. A.; Phillips, A. R.; Abu-Rmaileh, R.; Dickinson, P. A.; Abrahamsson, B.; Ostergaard, J.; Mullertz, A. Oral bioavailability of cinnarizine in dogs: relation to SNEDDS droplet size, drug solubility and in vitro precipitation. *Eur. J. Pharm. Sci.* **2013**, *48* (1–2), 339–50.
- (30) Sassene, P. J.; Knopp, M. M.; Hesselkilde, J. Z.; Koradia, V.; Larsen, A.; Rades, T.; Müller, A. Precipitation of a poorly soluble model drug during in vitro lipolysis: Characterization and dissolution of the precipitate. *J. Pharm. Sci.* **2010**, *99* (12), 4982–4991.
- (31) di Cagno, M.; Luppi, B. Drug “supersaturation” states induced by polymeric micelles and liposomes: A mechanistic investigation into permeability enhancements. *Eur. J. Pharm. Sci.* **2013**, *48* (4–5), 775–780.
- (32) Hofmann, A. F. Micellar Solubilization of Fatty Acids and Monoglycerides by Bile Salt Solutions. *Nature* **1961**, *190* (4781), 1106–1107.
- (33) O'Reilly, J. R.; Corrigan, O. I.; O'Driscoll, C. M. The effect of mixed micellar systems, bile salt/fatty acids, on the solubility and intestinal absorption of clofazimine (B663) in the anaesthetised rat. *Int. J. Pharm.* **1994**, *109* (2), 147–154.
- (34) Kleberg, K.; Jacobsen, J.; Müller, A. Characterising the behaviour of poorly water soluble drugs in the intestine: application

of biorelevant media for solubility, dissolution and transport studies.

*J. Pharm. Pharmacol.* **2010**, *62* (11), 1656–1668.

(35) Maldonado-Valderrama, J.; Wilde, P.; Macierzanka, A.; Mackie, A. The role of bile salts in digestion. *Adv. Colloid Interface Sci.* **2011**, *165* (1), 36–46.

(36) Gallier, S.; Ye, A.; Singh, H. Structural changes of bovine milk fat globules during in vitro digestion. *J. Dairy Sci.* **2012**, *95* (7), 3579–3592.

(37) FDA. Generally recognized as safe determination for medium-chain triglycerides when added directly to human food; GRAS Notices, GRN No. 449, 2014.

(38) Łoś-Rycharska, E.; Kieraszewicz, Z.; Czerwionka-Szaflarska, M. Medium chain triglycerides (MCT) formulas in paediatric and allergological practice. *Przegl. Gastroenterol.* **2016**, *11* (4), 226–231.

(39) Jandacek, R. J., Structured lipids: An overview and comments on performance enhancement potential. In *Food Components to Enhance Performance: An Evaluation of Potential Performance-Enhancing Food Components for Operational Rations*; M.Marriott, B., Ed.; National Academy Press: Washington, D.C., 1994.